Volume 9 | Number 16 | 21 August 2022

ORGANIC CHEMISTRY

FRONTIERS

CCS 中国化学会 CHINESE CHEMICAL SOCIETY
SIOC 1950
ROYAL SOCIETY OF CHEMISTRY
rsc.li/frontiers-organic

ORGANIC CHEMISTRY FRONTIERS

CCS 中国化学会 CHINESE CHEMICAL SOCIETY

SIOC 1950

ROYAL SOCIETY OF CHEMISTRY

RESEARCH ARTICLE

View Article Online
View Journal | View Issue

Cite this: *Org. Chem. Front.*, 2022, **9**, 4238

Photomodulation of ultrastable host–guest complexes in water and their application in light-controlled steroid release†

Patrícia Máximo, [a] Miriam Colaço, [a] Sofia R. Pauleta, [b,c] Paulo J. Costa, [d] Uwe Pischel, [e] A. Jorge Parola *[a] and Nuno Basílio *[a]

Received 15th March 2022,
Accepted 11th April 2022

DOI: 10.1039/d2qo00423b

rsc.li/frontiers-organic

The cucurbit[8]uril (CB8) synthetic receptor is shown to form high-affinity host–guest complexes with dicationic dithienylethene (DTE) photoswitches in water. ITC experiments combined with computational studies suggest that the formation of the inclusion complexes is mainly driven by a combination of hydrophobic effects, ion–dipole, hydrogen- and chalcogen-bonding interactions. The binding affinities were observed to be much higher for the DTE closed isomers, reaching values in the picomolar range (up to 10^{11} M^{-1}) while the open isomers display up to 10 000-fold lower affinities, setting ideal conditions for the development of robust photoswitchable host–guest complexes. The light-responsive affinity of these photoswitches toward CB8 was explored to control the encapsulation and release of nanomolar affinity steroids *via* competitive guest replacement.

Introduction

The use of affinity tools based on biological receptors, such as antibodies, aptamers, or the well-known biotin–avidin affinity pair, finds widespread applications in biology, medicine, nanotechnology, and related fields.[1–5] These include diagnosis, therapeutics, bioassays, imaging, bioconjugation, and purification, to give some examples. All these important applications arise from the ability of these macromolecules to recognize their targets with high selectivity and affinity (typically at or below the nanomolar range) under biologically relevant conditions. The design of synthetic receptors that match the extraordinary performance displayed by biological receptors is one of the major challenges of supramolecular chemistry.[6–9] In this context, several families of water-soluble high-affinity synthetic receptors have been reported, which include tetralactam macrocycles, pillararenes, tricyclic cyclophane receptors, and prominently cucurbit[*n*]urils (CBn).[10–16] CBn are barrel-shaped macrocyclic containers that comprise a hydrophobic and nonpolarizable cavity and two symmetric high-electron density carbonyl-fringed portals. Preferred guests of CBn are complementary to the host in shape, size and electronic properties,[17–19] providing inclusion complexes that may achieve binding constants as high as $K = 10^{17}$ M^{-1} in aqueous solution.[16]

Based on their high affinities towards specific guest molecules, CBn have been employed to develop exciting applications that include chemosensors for biologically relevant analytes, assays for enzymatic activity and membrane permeation, supramolecular bioconjugation, modulation of biomolecule self-assembly, bioimaging, supramolecular polymers, surface functionalization, and supramolecular organic frameworks.[20–32] Many of these applications benefit from the inherent reversibility and stimuli-responsive properties of host–guest binding pairs that allow control over the stability and/or structure of assemblies with chemical and/or physical stimuli.[33–35] Photoresponsive host–guest systems are particularly attractive because light presents appealing advantages such as remote activation and high spatial and temporal control, and, under ideal conditions, does not generate chemical byproducts.[36–38] The majority of so far reported light-responsive CBn host–guest complexes displays binding constants in the 10^6 M^{-1} range, *i.e.*, micromolar affinity.[39–46] Few

[a]*Laboratório Associado para a Química Verde (LAQV), Rede de Química e Tecnologia (REQUIMTE), Departamento de Química, Faculdade de Ciências e Tecnologia, Universidade NOVA de Lisboa, 2829-516 Caparica, Portugal. E-mail: ajp@fct.unl.pt, nuno.basilio@fct.unl.pt*

[b]*Associate Laboratory i4HB – Institute for Health and Bioeconomy, NOVA School of Science and Technology, Universidade NOVA de Lisboa, 2829-516 Caparica, Portugal*

[c]*Microbial Stress Lab, UCIBIO – Applied Molecular Biosciences Unit, Department of Chemistry/Department of Life Sciences, NOVA School of Science and Technology, Universidade NOVA de Lisboa, 2829-516 Caparica, Portugal*

[d]*BioISI – Biosystems & Integrative Sciences Institute, Faculty of Sciences, University of Lisboa, 1749-016 Lisboa, Portugal*

[e]*CIQSO – Centre for Research in Sustainable Chemistry and Department of Chemistry, University of Huelva, Campus de El Carmen s/n, E-21071 Huelva, Spain*

†Electronic supplementary information (ESI) available. See DOI: https://doi.org/10.1039/d2qo00423b

reports on all-photonically switchable dithienylethenes (DTEs) as guests of CBn are known, at best reaching nanomolar affinity with cucurbit[8]uril (CB8).[47–52] This eight-membered ring CBn homologue is known for its ability to simultaneously encapsulate two aromatic guests, and this binding process is particularly effective when complementary guests experience enhanced attractive interactions inside the macrocycle cavity.[17–19,53–55] Considering these binding properties, small substituents attached to the DTE core, such as *N*-methylpyridinium, seem to be required to ensure 1 : 1 binding stoichiometries while larger π-conjugated donor–acceptor moieties (*e.g.* styryl-pyridinium or *N*-phenyl-bipyridinium) usually lead to the formation of CB8 : DTE supramolecular polymers.[47–52] In the context of photocontrolling ultrastable CBn host–guest complexes ($K \geq 10^{10}$ M^{-1}) it is highly interesting to design DTE guests with improved binding capabilities, corresponding to picomolar affinity and a pronounced differential binding of the isomeric switch forms. To this end we designed a series of dicationic DTE derivatives, shown in Scheme 1. The rationale was based on the positional variation of positively charged *N*-methyl ammonium groups and hydrophobic surface areas, all of them being generally known to affect the stability of CBn-based host–guest complexes.[17–19] Gratifyingly, we could demonstrate that the closed isomers of some of the inspected DTEs display binding constants towards CB8 that reach values higher than 10^{11} M^{-1}, while the respective open isomers show up to four orders of magnitude lower affinities. The host–guest complexation was investigated through a combination of experimental and computational techniques, suggesting that non-classical hydrophobic effects, together with ion–dipole, hydrogen bonding and unprecedented chalcogen bonding interactions, are the main driving forces for the formation of the inclusion complexes.

The high selectivity and affinity of CB8 towards the closed DTE forms meet the requirements for the development of robust photoresponsive host–guest complexes, which even enable control over the encapsulation and release of ultrastable-binding guests of CB8. Steroids, known to form CB8 complexes with nanomolar affinity,[56] were chosen to benchmark the unprecedented potential of the herein investigated DTE guests. It is noteworthy that the all-photonic switching of the DTEs not only enables the release of steroids, but also pro-

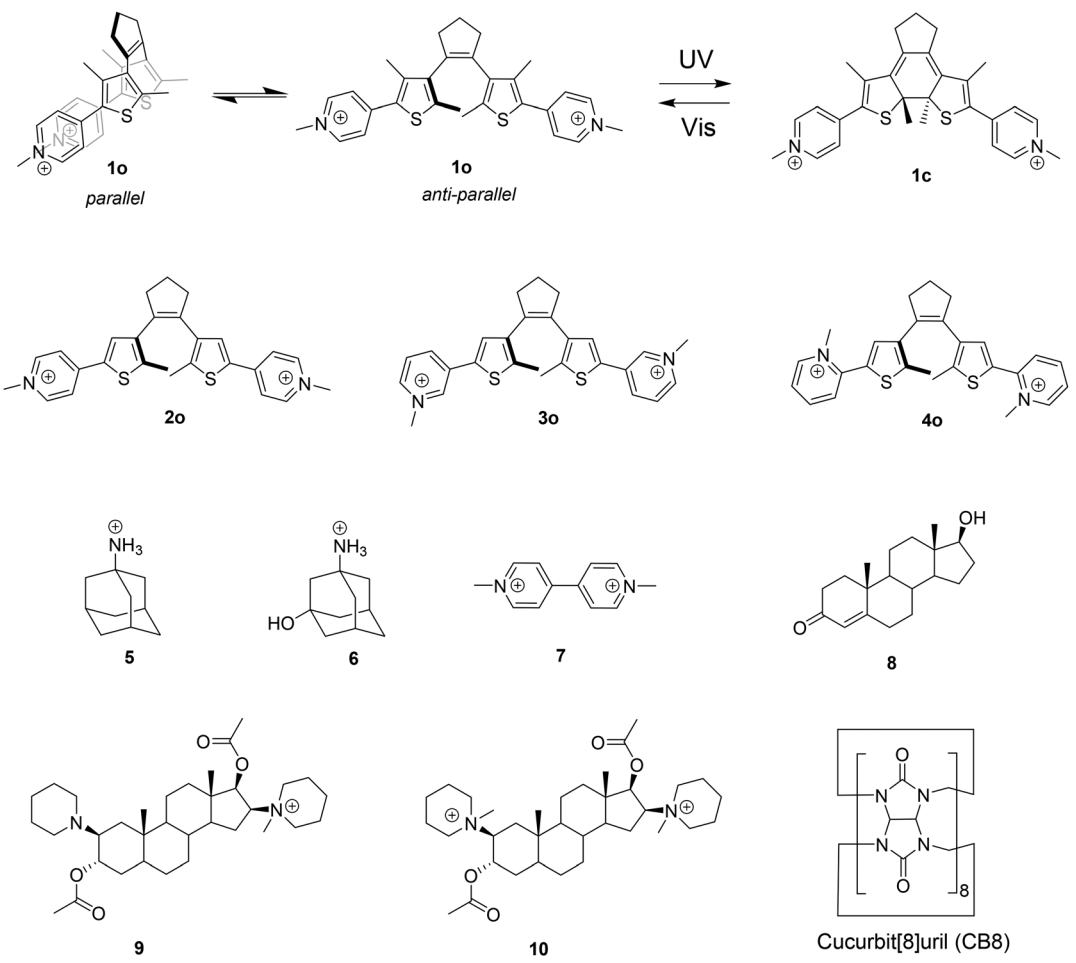

Scheme 1 Structures of the compounds investigated in this work. The DTE photoswitches were isolated as iodide salts; the solutions of adamantane and methyl viologen competitors **5**, **6**, and **7** were prepared from chloride salts and steroids **9** and **10** from bromide salts.

vides a means to sequester them by stimulation with low-energy visible light. These features were up to now elusive to other known photoswitchable host–guest pairs.

Results and discussion

DTE photoswitches interconvert between open (**o**) and closed (**c**) isomers upon irradiation with UV and visible/near-infrared light, as exemplified in Scheme 1 for DTE **1**. These compounds are known as P-type photochromes on account of their high thermal stability.[57] The open isomers are known to interconvert between the photochemically active antiparallel and inactive parallel conformations (see Scheme 1). The conformational equilibrium is known to limit the photocyclization quantum yield in an extension that is proportional to the relative population of the parallel conformer.[57]

To investigate the formation of inclusion complexes between CB8 and DTE derivatives we designed a set of four candidates (Scheme 1). This choice allows for a systematic study of the effect of changing the distance between the two formal positive charges from *para* (**2**) to *meta* (**3**) and *ortho* (**4**) positions. DTE **1** is included to inspect the influence of a larger hydrophobic surface area. In addition, the presence of extra methyl groups in the thiophene rings is expected to slow down the rate of interconversion between the parallel and antiparallel conformations of the open isomer, making it slow on the NMR chemical shift time scale.[58] This is important to demonstrate the exclusive inclusion of one of the conformers in the CB8 cavity.

Structural characterization

The formation of the inclusion complexes between CB8 and the DTE guests in their open (**o**) and closed (**c**) forms was first investigated by ^{1}H NMR spectroscopy. Fig. 1 shows, as a representative example, the ^{1}H NMR spectra of **1o**/**1c** in the absence and presence of 1 equiv. of CB8. As can be observed, the open **1o** and closed **1c** forms can be quantitatively interconverted upon irradiation with appropriate wavelengths. It is worth noting that the ^{1}H NMR spectrum of the open form **1o** shows split signals for protons c and e, and, is more noticeable, for the methyl protons d and g. This observation can be assigned to the slow exchange, on the NMR chemical-shift time scale, between the parallel and antiparallel conformations (see NOESY in the ESI, Fig. S24†). According to Irie and co-workers, the upfield signal of protons g is assigned to the antiparallel conformer and the downfield signal to the parallel conformer.[58] For DTE **1o**, the integration of the ^{1}H NMR signals

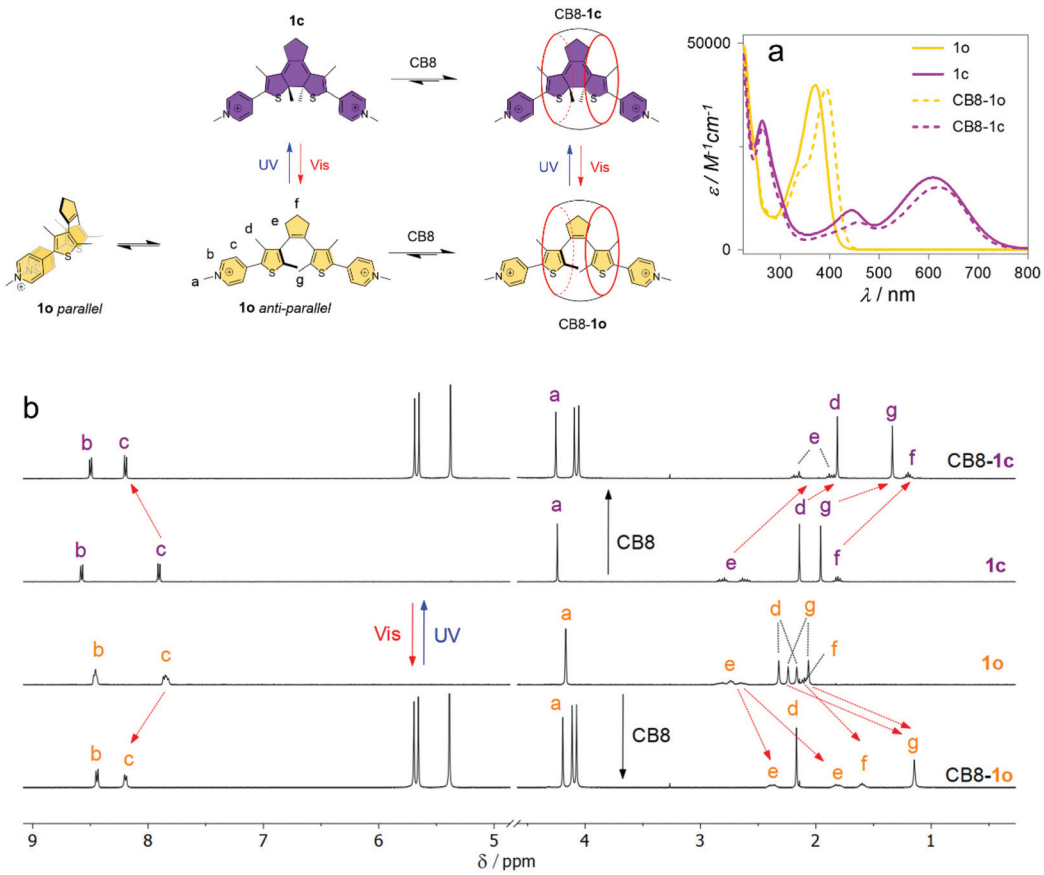

Fig. 1 (a) UV-Vis and (b) ^{1}H NMR (400 MHz) spectra of **1o**/**1c** in the absence and presence of 1 equiv. of CB8, at 25 °C. The NMR experiments were performed in D_2O at a 0.5 mM concentration while the UV-Vis spectra were acquired using concentrations of 20 μM in water.

shows a ratio of 54 : 46, slightly favoring the antiparallel conformation. Upon addition of 1 equiv. of CB8, the equilibrium is quantitatively shifted to the antiparallel conformer, which was confirmed by the observation of ROE cross signals for the protons d and g in the ROESY spectrum (see ESI, Fig. S25†). This is traced back to the preferential inclusion of this conformer in the CB8 cavity. The complexation-induced chemical shifts of both **1o** and **1c** indicate that the signals of the protons of the DTE core (d, e, f, and g) are displaced to a higher field, suggesting that the DTE core is deeply immersed in the hydrophobic cavity of the host. On the other hand, the signal assigned to the pyridinium protons c is shifted to a lower field, indicating the formation of C–H···O=C hydrogen bonding interactions between these protons and the carbonyl oxygens of the host.[59] It is noteworthy that the signals corresponding to the methyl d protons for the open form **1o** are less upfield shifted (−0.15 ppm) than those from the closed form **1c** (−0.33 ppm), corroborating a more efficient inclusion of the DTE core for the closed isomer.

^{1}H NMR experiments for the guests **2**,[47] **3**, and **4** show that the binding mode is similar for all DTEs (see ESI, Fig. S28 and S29†). However, in contrast to **1o** and **2o**,[47] **3o** and **4o** are not quantitatively converted into the respective closed isomers upon irradiation with 365 nm light. The integration of the ^{1}H NMR signals shows 46% and 80% of conversion into the closed forms for **3o** and **4o**, respectively. Complexation with CB8 significantly improves the photochemical performance of these photoswitches leading to photoconversion yields of 90% for **3o** → **3c** and 100% for **4o** → **4c**, upon irradiation at 365 nm.

To gain further insight into the structural features of the CB8 : DTE host–guest systems, semiempirical tight-binding calculations combined with a *meta*-dynamics driven search algorithm,[60] followed by DFT calculations (ωB97X-D functional), were performed (see the ESI†). This procedure yielded an ensemble of low-energy conformers for all host–guest systems, comprising the DTE core deeply inserted into the hydrophobic cavity of the CB8 host (Fig. S15–S18†), being coincident with the NMR results (see above). A subsequent DFT optimization of the lowest-energy inserted conformer of each system shows only subtle differences in the binding modes of the different guests (see ESI, Fig. S19†). This is supported by the observation of a reasonable overlap of the inserted DTE moiety along with a significant distortion of the CB8 cavity from the D_{8h} symmetry of the free host. In the particular case of DTE **1** (Fig. 2, top), the extra methyl groups point outwards the CB8 inner hydrophobic cavity at or slightly above the plane defined by the carbonyl oxygen atoms, being in agreement with the smaller complexation-induced upfield ^{1}HNMR shifts (see above).

Further analysis was performed with the Independent Gradient Model (IGM)[61,62] to identify key non-covalent interactions between CB8 and the DTE guests. This approach shows several weak contacts, depicted as green-colored isosurfaces in Fig. 2 (bottom) between the included DTE core and the concave cavity of the host, which are typically ascribed to van der Waals (vdW) interactions within this analysis scheme. There is also evidence for the presence of –N–Me$^+$···O=C interactions along with strong C–H···O=C interactions (Fig. 2, blue dashes and bluish green isosurfaces) which are common in CBn host–guest systems.[15,17,18,59,63,64] The latter interactions are present regardless of the position of the –N–Me group while the former appears to increase from **2** to **4**, as the formal charge increasingly approaches the C=O groups in the host–guest systems. This is also supported by the ^{1}H NMR experiments showing increasing downfield shifts for the N–Me protons a on going from **2** to **4** (see Fig. 1 and Fig. S28 and S29 in the ESI†).

A striking feature of the IGM analysis is the presence of C–S···O=C signatures, concomitant with short S···O contacts, as shown in Fig. 2 (orange dashes) for CB8 : **1o** and CB8 : **1c**, which can be assigned to chalcogen bonds.[65] These interactions are also observed in the other herein investigated host–guest systems (Fig. S20–S22 and Table S1 in the ESI†). Additionally, this is also the first report of chalcogen bonding[66,67] in a host–guest system featuring CBn, in parallel to the reported inclusion of molecular bromine and iodine in CB6 by halogen bonding.[68] These interactions are ascribed to the existence of a region of depleted electron density opposite to the R–Ch bond (Ch is a chalcogen atom), called a σ-hole.[69] Indeed, both closed and open forms of the DTE derivatives show maximum values of the electrostatic potential (V_{max}), which is associated with the presence of σ-holes (see Fig. S23 and Table S1 in the ESI†). Typically, the open forms possess four maxima as each thiophene ring has two σ-holes on the extension of the C–S bonds, while for closed forms, only three σ-holes are observed due to the coalescence of the maxima opposed to the pyridinium. For the specific case of **3o** and **3c**, the maximum located on the side of the pyridinium substituent could not be unequivocally discriminated from the one arising from N–Me$^+$.

Both complexes CB8 : **1c** (Fig. 2) and CB8 : **4c** (Fig. S23†) completely fulfill the commonly used criteria for classical chalcogen bonding, namely S···O distances less than the sum of vdW radii (<3.39 Å)[70] and C–S···O angles of 150–180°[71] (see Table S1 in the ESI†). The other complexes express similar tendencies with chalcogen bonding signatures clearly visible in the IGM analysis. However, some of the geometrical parameters slightly deviate from these stringent criteria, an observation that is rationalized by the constrained environment inside the CB8 host, as noted previously for the case of halogen-bonding guests of CBn.[68]

Binding affinity and selectivity

UV-Vis absorption spectroscopy. As can be observed from Fig. 3, the UV-Vis absorption spectroscopy titrations of **1o** and **1c** with CB8 show clean isosbestic points accompanied by a red shift of the lower energy bands. The UV-Vis absorption titration data hint at strong 1 : 1 binding ($K > 5 \times 10^6$ M^{-1}), characterized by a sharp leveling-off of the titration curves at 1 equiv. of host. Hence, competitive titrations were required to accurately extract such high binding constants. By using the

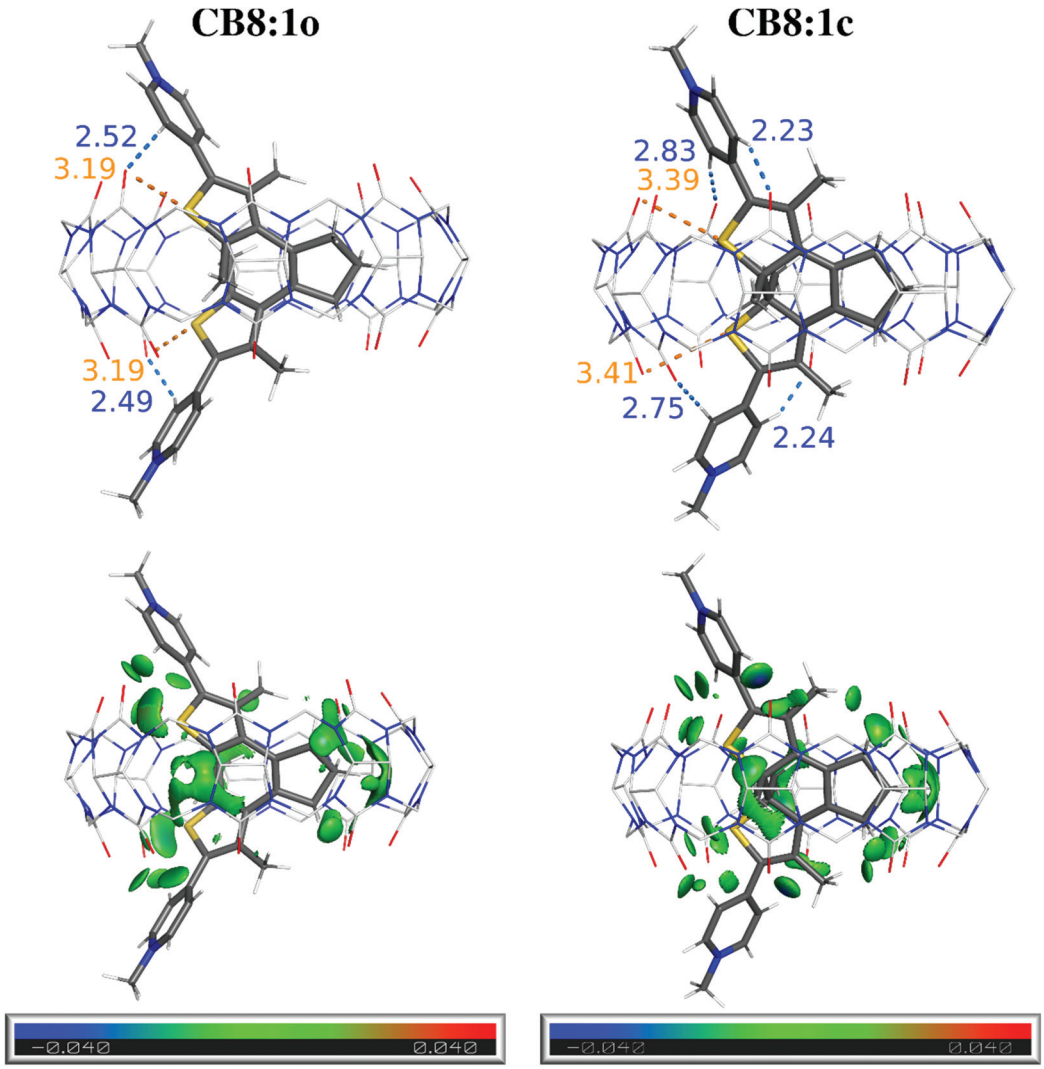

Fig. 2 Top: DFT-optimized structures (ωB97X-D/6-31G*; water) of CB8 : **1o** and CB8 : **1c** with the distances (Å) of the most relevant interactions shown in orange (S···O) or blue (C–H···O). Bottom: IGM analysis using a δg^{inter} isosurface of 0.008 a.u. and a BGR color code in the range −0.040 < ρ sign (λ_2) < 0.040 a.u.

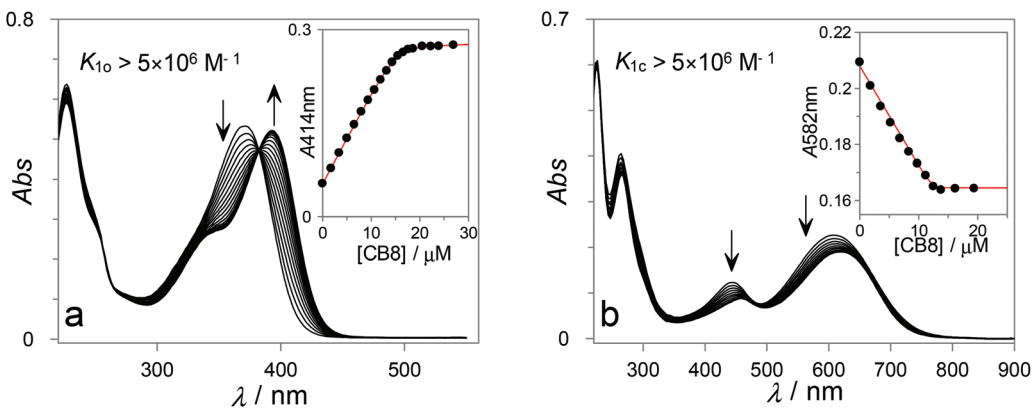

Fig. 3 (a) Spectral changes observed upon gradual addition of CB8 to a solution of **1o** (15 μM in H_2O). (b) The same for **1c** (13 μM in H_2O). In both cases, the data were successfully fitted to a 1 : 1 host–guest model.

adamantane derivatives **5** ($K_5 = 2.7 \times 10^9$ M^{-1}) and **6** ($K_6 = 1.4 \times 10^7$ M^{-1}) as competitor guests, values of $K_{1o} = 6.5 \times 10^6$ M^{-1} and $K_{1c} = 2.2 \times 10^{10}$ M^{-1} (see ESI, Fig. S1†) were obtained.

Similar experiments were performed for DTEs **3** and **4** (see ESI, Fig. S2–S4†), which also form high-affinity 1 : 1 complexes with CB8 and show comparable spectroscopic properties upon complexation. The results, along with previously reported data for DTE **2**,[47] are summarized in Table 1. From the analysis of the binding constants reported in Table 1, immediate conclusions can be drawn. First, all DTE guests show higher selectivity for the closed form, with the pronounced differential binding observed for **4** ($K_{4c}/K_{4o} > 10\,000$) being particularly impressive. It is also worth mentioning that the closed isomers of both **1** and **3** show 3 orders of magnitude higher affinity for CB8 than their open isomer counterparts, which is above the selectivity (*ca.* 100-fold) previously observed for DTE **2**.[47] Second, the absolute magnitude of the binding constants, observed for the closed isomers of the studied DTEs, is highly significant, reaching picomolar affinities for both **3c** and **4c** and subnanomolar affinities for **1c** and **2c**. The picomolar affinities reported here for the recognition of photoswitchable compounds with synthetic receptors in aqueous solution are unprecedented and, together with the selectivity observed for the closed *versus* open isomers, unlock attractive possibilities for their exploitation in the development of stimuli-responsive supramolecular systems (see below).

Isothermal titration calorimetry. In addition to the spectroscopic binding studies discussed above, we have conducted isothermal titration calorimetry (ITC) experiments to gain further thermodynamic insight into the complexation of the DTE photoswitches with CB8. Anticipating the high binding constants based on the UV-Vis absorption titration results, competitive ITC experiments were performed in most cases, except for **1o** and **4o** which were analyzed by direct titrations. Methyl viologen **7** and 1-adamantyl ammonium **5** were chosen as competitor guests because they are known to form defined 1 : 1 complexes with CB8, facilitating the quantitative analysis of the competitive binding. ITC experiments of **7** and **5** with CB8 (see ESI, Fig. S8–S10†) yielded binding constants, enthalpy (ΔH) and entropy (ΔS) changes that are in excellent agreement with previously published data (Table 2).[47,72]

Fig. 4 shows two representative examples of the data obtained from the ITC titration experiments with DTE switches. The results shown in Fig. 4a correspond to the direct titration of CB8 with **1o**, while Fig. 4b shows the results obtained for the competitive replacement of **7** from the CB8 cavity by **1c**. Similar experiments were conducted for the other DTE guests (see ESI, see Fig. S11–S14†). However, in the cases of **3** and **4** it was not possible to obtain ITC results for the closed isomers since they could not be generated quantitatively by the irradiation of the respective open DTEs (see above). The ITC thermodynamic data are compiled in Table 2. Gratifyingly, the obtained binding constants are in excellent agreement with those from the UV-Vis spectroscopic titrations (see Table 1).

Table 2 Thermodynamic data obtained by ITC for the formation of CB8 complexes with DTEs **1–4**, adamantyl ammonium **5** and methyl viologen **7** guests

	K/M^{-1}	ΔG/kJ mol^{-1}	ΔH/kJ mol^{-1}	$-T\Delta S$/kJ mol^{-1}
1o[a]	6.5×10^6	−38.9	−41.8	2.9
2o[b]	6.7×10^7	−44.7	−39.5	−5.2
3o[b]	1.6×10^8	−46.7	−44.7	−2.0
4o[a]	1.0×10^7 [d]	−40.0	−36.5	−3.5
1c[b]	2.2×10^{10}	−59.0	−63.7	4.7
2c[b]	4.7×10^9	−55.2	−56.1	0.9
3c[c]	—	—	—	—
4c[c]	—	—	—	—
5[b]	2.5×10^9	−53.6	−34.3	−19.3
7[a]	5.7×10^6	−38.6	−25.2	−13.4

[a] Obtained by direct ITC experiments. [b] Obtained by a competitive replacement experiment using **7** as a competitor. [c] Not investigated due to the presence of both closed and open forms at the photostationary state. [d] This K value falls between the higher limit to be accurately measured by direct titrations but not high enough to be measured with the competitor **7** by ITC.

The thermodynamic parameters show that for all DTEs, both as closed and open isomers, the formation of the host–guest complexes is enthalpically driven. It can be inferred that the release of high-energy water molecules from the CB8 hydrophobic cavity and from the guest hydrophobic surface is the main reason for this observation.[73] In addition, ion–dipole, hydrogen- and chalcogen-bonding interactions between the positively charged guests and the electronegative CB8 portals are deemed to contribute to the binding enthalpy, albeit to a lesser extent due to the enthalpic penalty associated with the desolvation of the highly polar/charged surfaces.[74]

On the one hand, regarding the open isomers, a moderate 10-fold higher affinity of CB8 towards **2o** in comparison with

Table 1 Binding constants (K), selectivity (K_{closed}/K_{open}), photochemical quantum yields (QY) and photostationary state (PSS) composition

	K_{open} [a]/M^{-1}	K_{closed} [a]/M^{-1}	K_{closed}/K_{open}	$QY_{o\rightarrow c}$ free/complex	% closed at PSS free/complex	$QY_{c\rightarrow o}$ [e] free/complex
1	6.5×10^6	2.2×10^{10}	3.4×10^3	0.04[c]/0.14[c]	100[c]/100[c]	0.001/0.001
2[b]	5.4×10^7	6.2×10^9	1.1×10^2	0.04[c]/0.32[c]	100[c]/100[c]	0.0003/0.0003
3	1.0×10^8	1.5×10^{11}	1.5×10^3	0.003[d]/0.011[d]	61[d]/95[d]	0.0014/0.0010
4	1.9×10^7	2.1×10^{11}	1.1×10^4	0.009[d]/0.087[d]	70[d]/100[d]	0.0058/0.0054

[a] Maximum estimated error of 20%. [b] Data previously reported in ref. 47. [c] Irradiation at 365 nm. [d] Irradiation at 334 nm; these data are dependent on the irradiation wavelength and different closed/open ratios can be observed when the irradiation of these compounds is carried out at 365 nm (see text). [e] Irradiation at 550 nm.

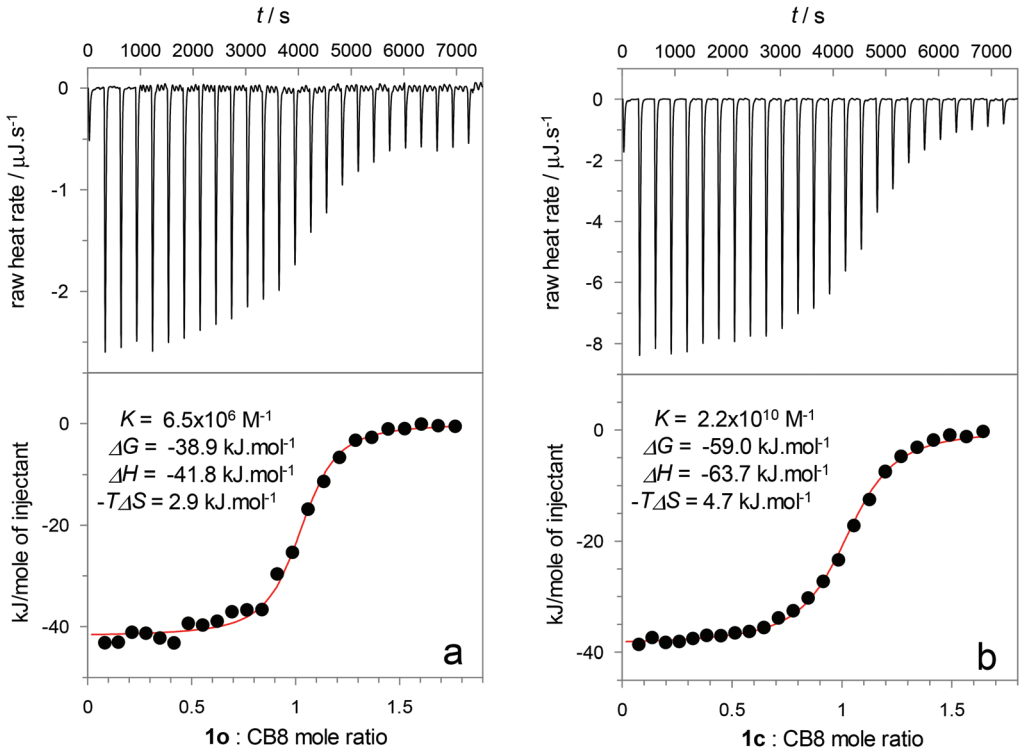

Fig. 4 Isotherms for the (a) titration of DTE **1o** (138 μM) into CB8 (22.5 μM) and (b) for the competitive titration of DTE **1c** (570 μM) into a CB8 solution (100 μM) containing 5000 μM methyl viologen **7**. The data fitting for the experiment (b) was achieved using a competitive replacement model with the CB8 : **7** binding constant (K_7 = 5.7 × 10^6 M^{-1}) and enthalpy variation (ΔH = −25.2 kJ mol^{-1}) set as constants. Both titrations were performed in water at 25 °C.

the more crowded **1o** was observed. This can be tentatively attributed to entropic factors, related to the lower conformational flexibility of **1o** inside the host cavity. On the other hand, when comparing the closed isomers, the enthalpic changes show that **1c** displays a slightly more negative enthalpy change ($\Delta\Delta H$ = −7.6 kJ mol^{-1}) than **2c** which may be related to the larger hydrophobic surface of the former, releasing more "frustrated" water molecules from the solvation shell of the guest. It should be noted that the structural studies (see above) show that the extra methyl groups of **1** are not included in the inner hydrophobic cavity, and thus, can hardly contribute to a more efficient release of high-energy water molecules from the CB8 inner cavity.

The most intriguing results are related to the comparison between the open and closed isomers of **1** and **2**. Generally speaking, it is clearly evident from the ITC data that the considerably higher affinity observed for closed DTE isomers towards CB8 arises exclusively from their more favorable binding enthalpy. This is surprising since the most obvious reason for the preferential complexation of closed DTE isomers is guest preorganization which is traditionally accepted as an entropic phenomenon. However, examples of this "entropic paradox" were previously reported for ligand–protein complexes challenging the common understanding of host–guest binding energetics.[75] The reasons for the lower enthalpic variation observed for the open isomers may be assigned to different factors. The parallel/antiparallel conformational exchange in the open forms is one contributor. Based on the enthalpy-driven association of aromatic dyes, Würthner and co-workers have suggested that high-energy frustrated water molecules may also be found at hydrophobic π-surfaces.[76] In this context, the open isomers may adopt a parallel conformation to decrease the non-polar surface area exposed to the solvent and therefore reduce the number of high-energy water molecules that are released upon binding. In fact, the stabilization of the photochemically inactive parallel conformation in more polar solvents has been considered to rationalize the reduced photochemical reactivity in these media.[57]

Photochemistry. The photochemical properties of the DTE photoswitches and their CB8 inclusion complexes were investigated in detail by UV-Vis absorption spectroscopy (see the ESI†). Fig. 1a (and Fig. S33 in the ESI†) showcases the spectral variations observed upon irradiation of **1o**, at 365 nm, in the presence and absence of CB8. As can be observed, the band centered at 370 nm (or at 395 nm for the complex) decreases and a new band in the visible region appears due to the photocyclization of **1o** into the more conjugated form **1c**. The transformation is quantitative, as established by NMR (see above), and the quantum yield is improved from $\phi_{o\text{–}c}$ = 0.04 to $\phi_{o\text{–}c}$ = 0.14 upon encapsulation of **1o** into the cavity of CB8 due, at least in part, to the preorganization of the DTE in the photo-

chemically active antiparallel conformation.[47,58,77] This trend is consistently observed for all DTEs herein investigated (see Table 1 and ESI†), being most significant for compounds **2** and **4**, for which the ϕ_{o-c} increases 8.0 and 9.7 times, respectively. The ^{1}H NMR experiments for **1o** showed a 2-fold increase of the photochemically active antiparallel conformation upon encapsulation by CB8 (see above) which confirms the observed trend of the quantum yield improvement (3.5-fold). However, it is obvious that this is likely not the only reason for the increased efficiency of the photoinduced electrocyclization reaction. The inclusion of the DTEs in the cavity of CB8 may extend the lifetime of the excited state by the restriction of the rotational and vibrational freedom, thereby contributing to the observed increase of the ϕ_{o-c}.[78] In contrast to the photocyclization, the photocycloreversion quantum yields remain practically unaffected by the CB8 complexation in line with the more rigid and conformationally more restricted character of the closed DTE isomers.

Light-controlled catch and release of high-affinity binding steroids. CB8 was previously demonstrated to bind steroids with high affinity in aqueous solution.[56] The best binders include the hormone testosterone **8** and neuromuscular blockers vecuronium **9** and pancuronium **10**. Their affinities are situated in between the ones for the open and closed DTE photoswitches that were investigated in this work. This provides ideal conditions to explore the light-controlled catch and release of these guests from the CB8 nanocontainer *via* the light-induced reversible formation of strong competitors. We have previously explored this strategy to demonstrate the release of biologically relevant guests from CBn and calixarene hosts but its application to highly challenging guests with nanomolar affinity and at physiological pH was never realized.[43–45,79,80] First, the binding constants of the investigated steroids were determined from UV-Vis competitive displacement assays using the DTEs as the indicator spectroscopic probe (see ESI, Fig. S5–S7†). From these studies, binding constants of $K_8 = 2.1 \times 10^8$ M^{-1}, $K_9 = 1.9 \times 10^{11}$ M^{-1} and $K_{10} = 3.6 \times 10^9$ M^{-1} were obtained for testosterone **8**, vecuronium **9**, and pancuronium **10**, respectively.

With the steroid binding constants in mind, DTE **4** was selected to demonstrate the control over the binding and release of pancuronium **10** by using light stimulation. As can be observed from the ^{1}H NMR spectra in Fig. 5, the CB8 : **10** complex is not significantly dissociated in the presence of 1.2 equivalents of DTE in the open form (**4o**) (see spectra (a) and (b) in Fig. 5) in good agreement with >100-fold selectivity of CB8 towards **10** ($K_{10} = 3.6 \times 10^9$ M^{-1} *vs.* $K_{4o} = 1.9 \times 10^7$ M^{-1}). Irradiation (365 nm) of the mixture directly in the NMR tube

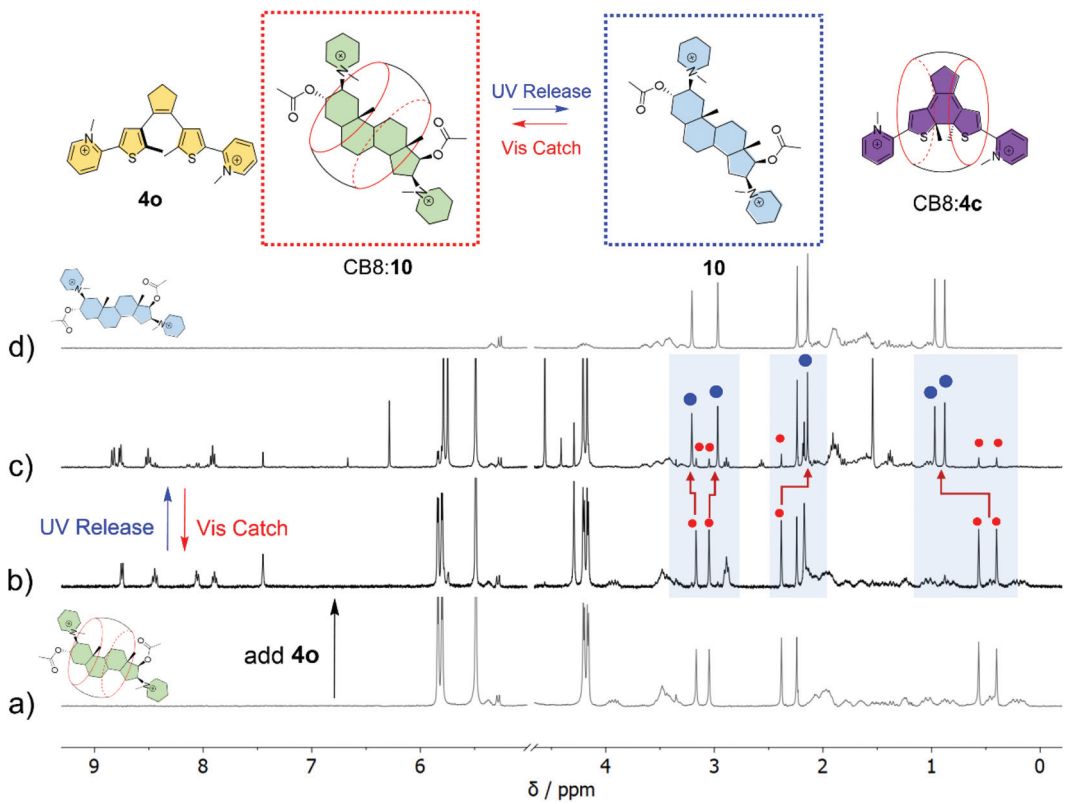

Fig. 5 ^{1}H NMR (400 MHz) experiments demonstrating the light-controlled binding and release of pancuronium **10** (see the schematic on top), using DTE **4** as a competitor with photocontrolled affinity. ^{1}H NMR spectra of (a) the CB8 : **10** host–guest complex (1 mM); (b) a solution containing CB8 (1 mM), **10** (1 mM) and DTE **4o** (1.2 mM); (c) the same as in (b) upon irradiation with 365 nm until reaching the PSS; and (d) ^{1}H NMR spectrum of **10** (1 mM). All solutions were prepared in D_2O and the spectra acquired at 298 K. Blue dots refer to free **10** and red dots symbolize signals of CB8-bound **10**.

leads to the formation of a closed DTE form (**4c**) with a PSS **4c** : **4o** composition of 83 : 17 under the concrete experimental conditions (note that this corresponds effectively to an equimolar concentration of **4c** with respect to **10** and CB8); see Fig. 5(c). As the photogenerated DTE **4c** is a stronger binder ($K_{\mathbf{4o}}$ = 2.1 × 10^{11} M^{-1}) than **4o**, it competes more effectively with **10** for the CB8 binding site, leading to the release of the steroid as can be demonstrated by the appearance of the ^{1}H NMR signals of free **10** (*ca*. 85%) in slow exchange with a small fraction of CB8 : **10** complex (*ca*. 15%), again in good agreement with the selectivity anticipated from the binding constants ($K_{\mathbf{10}}$ = 3.6 × 10^9 M^{-1} *vs*. $K_{\mathbf{4o}}$ = 2.1 × 10^{11} M^{-1}). Similar experiments using vecuronium **9** ($K_{\mathbf{9}}$ = 1.9 × 10^{11} M^{-1}) show a photoinduced steroid release of *ca.* 47% (see ESI, Fig. S31†). The photoinduced release of testosterone **8** ($K_{\mathbf{8}}$ = 2.1 × 10^8 M^{-1}), the primary sex hormone in males, was also demonstrated using DTE **1** (see the ESI†). The ^{1}H NMR results (see ESI, Fig. S32†) showed that the light-induced formation of **1c** from **1o** leads to *ca*. 80% release of testosterone **8** from CB8.

These experiments highlight the potential of the herein designed DTE photoswitches to be employed in the context of implementing photofunctionality in ultrastable host–guest assemblies. This is by no means trivial, as in fact no examples of photoactive guests with picomolar affinity for CB8 are known so far in the literature.

Conclusions

The rational design of photoswitchable DTE guests has led to the discovery of new ultrastable supramolecular pairs with picomolar affinity (K > 10^{11} M^{-1}) in aqueous solution. Our studies suggest that the formation of CB8 : DTE complexes is mainly driven by enthalpic hydrophobic effects. This is supplemented by ion–dipole interactions and hydrogen-bonding, which are frequently observed in CBn host–guest complexes, and so far in this context unexploited chalcogen-bonding interactions. The remarkable affinity of CB8 towards DTE photoswitches is accompanied by particularly impressive differential binding of the closed DTE isomers (K_c/K_o up to 10 000-fold). This is reasoned with a higher enthalpic gain upon binding of the closed form, which can be associated with the larger exothermic dehydration of the π-surface of these more rigid and flat closed DTE isomers.

The superior performance of the new switchable host–guest pairs was successfully exploited to trigger, *via* competitive binding, the release of tightly bound steroids from the CB8 cavity using light as a stimulus. This serves as an example for the application potential of the investigated systems. It is not difficult to predict that they may find further use, wherever external control by light is an advantage, such as in supramolecular affinity labeling, programmable soft materials, or drug delivery. In these contexts, the pH-independent, reversible, and all-photonic operation of CB8 : DTE pairs under physiological conditions constitutes a clear surplus.

Author contributions

P. M. synthesized the compounds and performed the chemical characterization. P. M., M. C. and S. R. P. conducted the spectroscopic and ITC experiments. P. J. C. performed the computational calculations. The experimental work was designed and supervised by N. B. and A. J. P. The manuscript was written by N. B. with contributions from P. J. C., A. J. P and U. P. All authors analyzed and discussed the results and reviewed the manuscript.

Conflicts of interest

There are no conflicts to declare.

Acknowledgements

This work was supported by the Associate Laboratory for Green Chemistry – LAQV (projects UIDB/50006/2020 and UIDP/50006/2020), the Research Unit on Applied Molecular Biosciences – UCIBIO (projects UIDP/04378/2020 and UIDB/04378/2020) and the Associate Laboratory Institute for Health and Bioeconomy – i4HB (project LA/P/0140/2020) which are financed by national funds from FCT/MCTES. FCT/MCTES is also acknowledged for supporting the National Portuguese NMR Network (ROTEIRO/0031/2013–PINFRA/22161/2016, cofinanced by FEDER through COMPETE 2020, POCI, PORL, and FCT through PIDDAC) and for the grants PTDC/QUI-COL/32351/2017 (NB), PTDC/QUI-QFI/30951/2017 (AJP), FCT-ANR/BBB-MET/0023/2012 (SRP), PTDC/BIA-BQM/29442/2017 (SRP), CEECIND/00466/2017 (NB) and 2021.07205.BD (MC). European Commission is acknowledged for the INFUSION project grant N. 734834 under H2020-MSCA-RISE-2016. PJC acknowledges FCT for the CEECIND 2021 Initiative (CEECIND/00381/2021) and strategic projects UIDB/04046/2020-UIDP/04046/2020 (BioISI). UP thanks the Spanish Ministry of Science and Innovation for financial support (project PID2020-119992GB-I00).

References

1 M. X. Sliwkowski and I. Mellman, Antibody Therapeutics in Cancer, *Science*, 2013, **341**, 1192–1198.
2 V. J. B. Ruigrok, M. Levisson, M. H. M. Eppink, H. Smidt and J. Van Der Oost, Alternative affinity tools: More attractive than antibodies?, *Biochem. J.*, 2011, **436**, 1–13.
3 J. D. Munzar, A. Ng and D. Juncker, Duplexed aptamers: history, design, theory, and application to biosensing, *Chem. Soc. Rev.*, 2019, **48**, 1390–1419.
4 M. R. Dunn, R. M. Jimenez and J. C. Chaput, Analysis of aptamer discovery and technology, *Nat. Rev. Chem.*, 2017, **1**, 0076.
5 H. M. Meng, H. Liu, H. Kuai, R. Peng, L. Mo and X. B. Zhang, Aptamer-integrated DNA nanostructures for

biosensing, bioimaging and cancer therapy, *Chem. Soc. Rev.*, 2016, **45**, 2583–2602.
6 L. Escobar and P. Ballester, Molecular recognition in water using macrocyclic synthetic receptors, *Chem. Rev.*, 2021, **121**, 2445–2514.
7 W. Liu, S. K. Samanta, B. D. Smith and L. Isaacs, Synthetic mimics of biotin/(strept)avidin, *Chem. Soc. Rev.*, 2017, **46**, 2391–2403.
8 D. Shetty, J. K. Khedkar, K. M. Park and K. Kim, Can we beat the biotin–avidin pair?: cucurbit[7]uril-based ultra-high affinity host–guest complexes and their applications, *Chem. Soc. Rev.*, 2015, **44**, 8747–8761.
9 C. L. Schreiber and B. D. Smith, Molecular conjugation using non-covalent click chemistry, *Nat. Rev. Chem.*, 2019, **3**, 393–400.
10 E. M. Peck, W. Liu, G. T. Spence, S. K. Shaw, A. P. Davis, H. Destecroix and B. D. Smith, Rapid Macrocycle Threading by a Fluorescent Dye–Polymer Conjugate in Water with Nanomolar Affinity, *J. Am. Chem. Soc.*, 2015, **137**, 8668–8671.
11 W. Liu, A. Johnson and B. D. Smith, Guest Back-Folding: A Molecular Design Strategy That Produces a Deep-Red Fluorescent Host/Guest Pair with Picomolar Affinity in Water, *J. Am. Chem. Soc.*, 2018, **140**, 3361–3370.
12 W. Xue, P. Y. Zavalij and L. Isaacs, Pillar[n]MaxQ: A New High Affinity Host Family for Sequestration in Water, *Angew. Chem., Int. Ed.*, 2020, **59**, 13313–13319.
13 W. Liu, C. Lin, J. A. Weber, C. L. Stern, R. M. Young, M. R. Wasielewski and J. F. Stoddart, Cyclophane-Sustained Ultrastable Porphyrins, *J. Am. Chem. Soc.*, 2020, **142**, 8938–8945.
14 W. Liu, S. Bobbala, C. L. Stern, J. E. Hornick, Y. Liu, A. E. Enciso, E. A. Scott and J. F. Stoddart, XCage: A Tricyclic Octacationic Receptor for Perylene Diimide with Picomolar Affinity in Water, *J. Am. Chem. Soc.*, 2020, **142**, 3165–3173.
15 M. V. Rekharsky, T. Mori, C. Yang, Y. H. Ko, N. Selvapalam, H. Kim, D. Sobransingh, A. E. Kaifer, S. Liu, L. Isaacs, W. Chen, S. Moghaddam, M. K. Gilson, K. Kim and Y. Inoue, A synthetic host-guest system achieves avidin-biotin affinity by overcoming enthalpy-entropy compensation, *Proc. Natl. Acad. Sci. U. S. A.*, 2007, **104**, 20737–20742.
16 L. Cao, M. Šekutor, P. Y. Zavalij, K. Mlinarić-Majerski, R. Glaser and L. Isaacs, Cucurbit[7]uril·Guest Pair with an Attomolar Dissociation Constant, *Angew. Chem., Int. Ed.*, 2014, **53**, 988–993.
17 S. J. Barrow, S. Kasera, M. J. Rowland, J. del Barrio and O. A. Scherman, Cucurbituril-Based Molecular Recognition, *Chem. Rev.*, 2015, **115**, 12320–12406.
18 K. I. Assaf and W. M. Nau, Cucurbiturils: from synthesis to high-affinity binding and catalysis, *Chem. Soc. Rev.*, 2015, **44**, 394–418.
19 E. Masson, X. Ling, R. Joseph, L. Kyeremeh-Mensah and X. Lu, Cucurbituril chemistry: a tale of supramolecular success, *RSC Adv.*, 2012, **2**, 1213–1247.
20 R. N. Dsouza, A. Hennig and W. M. Nau, Supramolecular Tandem Enzyme Assays, *Chem. – Eur. J.*, 2012, **18**, 3444–3459.
21 G. Ghale and W. M. Nau, Dynamically Analyte-Responsive Macrocyclic Host–Fluorophore Systems, *Acc. Chem. Res.*, 2014, **47**, 2150–2159.
22 L. Yang, X. Tan, Z. Wang and X. Zhang, Supramolecular Polymers: Historical Development, Preparation, Characterization, and Functions, *Chem. Rev.*, 2015, **115**, 7196–7239.
23 J. Tian, L. Chen, D.-W. Zhang, Y. Liu and Z.-T. Li, Supramolecular organic frameworks: engineering periodicity in water through host–guest chemistry, *Chem. Commun.*, 2016, **52**, 6351–6362.
24 A. Kataki-Anastasakou, J. C. Axtell, S. Hernandez, R. M. Dziedzic, G. J. Balaich, A. L. Rheingold, A. M. Spokoyny and E. M. Sletten, Carborane Guests for Cucurbit[7]uril Facilitate Strong Binding and On-Demand Removal, *J. Am. Chem. Soc.*, 2020, **142**, 20513–20518.
25 F. Biedermann, G. Ghale, A. Hennig and W. M. Nau, Fluorescent artificial receptor-based membrane assay (FARMA) for spatiotemporally resolved monitoring of biomembrane permeability, *Commun. Biol.*, 2020, **3**, 383.
26 S. Sinn and F. Biedermann, Chemical Sensors Based on Cucurbit[n]uril Macrocycles, *Isr. J. Chem.*, 2018, **58**, 357–412.
27 M. J. Webber, E. A. Appel, B. Vinciguerra, A. B. Cortinas, L. S. Thapa, S. Jhunjhunwala, L. Isaacs, R. Langer and D. G. Anderson, Supramolecular PEGylation of biopharmaceuticals, *Proc. Natl. Acad. Sci. U. S. A.*, 2016, **113**, 14189–14194.
28 L. A. Logsdon and A. R. Urbach, Sequence-Specific Inhibition of a Nonspecific Protease, *J. Am. Chem. Soc.*, 2013, **135**, 11414–11416.
29 W. Li, A. T. Bockus, B. Vinciguerra, L. Isaacs and A. R. Urbach, Predictive recognition of native proteins by cucurbit[7]uril in a complex mixture, *Chem. Commun.*, 2016, **52**, 8537–8540.
30 A. T. Bockus, L. C. Smith, A. G. Grice, O. A. Ali, C. C. Young, W. Mobley, A. Leek, J. L. Roberts, B. Vinciguerra, L. Isaacs and A. R. Urbach, Cucurbit[7]uril–Tetramethylrhodamine Conjugate for Direct Sensing and Cellular Imaging, *J. Am. Chem. Soc.*, 2016, **138**, 16549–16552.
31 S. van Dun, C. Ottmann, L.-G. Milroy and L. Brunsveld, Supramolecular Chemistry Targeting Proteins, *J. Am. Chem. Soc.*, 2017, **139**, 13960–13968.
32 H. Yang, B. Yuan, X. Zhang and O. A. Scherman, Supramolecular Chemistry at Interfaces: Host–Guest Interactions for Fabricating Multifunctional Biointerfaces, *Acc. Chem. Res.*, 2014, **47**, 2106–2115.
33 A. E. Kaifer, Toward Reversible Control of Cucurbit[n]uril Complexes, *Acc. Chem. Res.*, 2014, **47**, 2160–2167.
34 L. Isaacs, Stimuli Responsive Systems Constructed Using Cucurbit[n]uril-Type Molecular Containers, *Acc. Chem. Res.*, 2014, **47**, 2052–2062.

35 K. M. Park, M. Y. Hur, S. K. Ghosh, S. Kim, D. R. Boraste and K. Kim, Cucurbit[n]uril-based amphiphiles that self-assemble into functional nanomaterials for therapeutics, *Chem. Commun.*, 2019, 10654–10664.

36 D.-H. Qu, Q.-C. Wang, Q.-W. Zhang, X. Ma and H. Tian, Photoresponsive Host–Guest Functional Systems, *Chem. Rev.*, 2015, **115**, 7543–7588.

37 P. Ceroni, A. Credi and M. Venturi, Light to investigate (read) and operate (write) molecular devices and machines, *Chem. Soc. Rev.*, 2014, **43**, 4068–4083.

38 Z. Yang, Z. Liu and L. Yuan, Recent Advances of Photoresponsive Supramolecular Switches, *Asian J. Org. Chem.*, 2021, **10**, 74–90.

39 F. Tian, D. Jiao, F. Biedermann and O. A. Scherman, Orthogonal switching of a single supramolecular complex, *Nat. Commun.*, 2012, **3**, 1207.

40 J. del Barrio, S. T. J. Ryan, P. G. Jambrina, E. Rosta and O. A. Scherman, Light-Regulated Molecular Trafficking in a Synthetic Water-Soluble Host, *J. Am. Chem. Soc.*, 2016, **138**, 5745–5748.

41 Y. V. Fedorov, S. V. Tkachenko, E. Y. Chernikova, I. a. Godovikov, O. a. Fedorova and L. Isaacs, Photoinduced guest transformation promotes translocation of guest from hydroxypropyl-β-cyclodextrin to cucurbit[7]uril, *Chem. Commun.*, 2015, **51**, 1349–1352.

42 A. Zubillaga, P. Ferreira, A. J. Parola, S. Gago and N. Basílio, pH-Gated photoresponsive shuttling in a water-soluble pseudorotaxane, *Chem. Commun.*, 2018, **54**, 2743–2746.

43 M. A. Romero, R. J. Fernandes, A. J. Moro, N. Basílio and U. Pischel, Light-induced cargo release from a cucurbit[8]uril host by means of a sequential logic operation, *Chem. Commun.*, 2018, **54**, 13335–13338.

44 N. Basílio and U. Pischel, Drug Delivery by Controlling a Supramolecular Host-Guest Assembly with a Reversible Photoswitch, *Chem. – Eur. J.*, 2016, **22**, 15208–15211.

45 M. A. Romero, N. Basílio, A. J. Moro, M. Domingues, J. A. González-Delgado, J. F. Arteaga and U. Pischel, Photocaged Competitor Guests: A General Approach Toward Light-Activated Cargo Release From Cucurbiturils, *Chem. – Eur. J.*, 2017, **23**, 13105–13111.

46 J. Wei, T. Jin, Y. Yin, X. Jiang, S. Zheng, T. Zhan, J. Cui, L. Liu, L. Kong and K. Zhang, Red-light-responsive molecular encapsulation in water: an ideal combination of photochemistry and host–guest interaction, *Org. Chem. Front.*, 2019, **6**, 498–505.

47 P. Ferreira, B. Ventura, A. Barbieri, J. P. Da Silva, C. A. T. Laia, A. J. Parola and N. Basílio, A Visible–Near–Infrared Light–Responsive Host–Guest Pair with Nanomolar Affinity in Water, *Chem. – Eur. J.*, 2019, **25**, 3477–3482.

48 M. Colaço, P. Máximo, A. Jorge Parola and N. Basílio, Photoresponsive Binding Dynamics in High–Affinity Cucurbit[8]uril–Dithienylethene Host–Guest Complexes, *Chem. – Eur. J.*, 2021, **27**, 9550–9555.

49 P. Remón, D. González, S. Li, N. Basílio, J. Andréasson and U. Pischel, Light-driven control of the composition of a supramolecular network, *Chem. Commun.*, 2019, **55**, 4335–4338.

50 D. Sun, Y. Wu, X. Han and S. Liu, Achieving Enhanced Photochromic Properties of Diarylethene through Host–Guest Interaction in Aqueous Solution, *Chem. – Eur. J.*, 2021, **27**, 16153–16160.

51 H. Wu, Y. Chen, X. Dai, P. Li, J. F. Stoddart and Y. Liu, In Situ Photoconversion of Multicolor Luminescence and Pure White Light Emission Based on Carbon Dot-Supported Supramolecular Assembly, *J. Am. Chem. Soc.*, 2019, **141**, 6583–6591.

52 G. Liu, Y. Zhang, C. Wang and Y. Liu, Dual Visible Light-Triggered Photoswitch of a Diarylethene Supramolecular Assembly with Cucurbit[8]uril, *Chem. – Eur. J.*, 2017, **23**, 14425–14429.

53 Z. Huang, X. Chen, G. Wu, P. Metrangolo, D. Whitaker, J. A. McCune and O. A. Scherman, Host-Enhanced Phenyl-Perfluorophenyl Polar–π Interactions, *J. Am. Chem. Soc.*, 2020, **142**, 7356–7361.

54 F. Biedermann, M. Vendruscolo, O. A. Scherman, A. De Simone and W. M. Nau, Cucurbit[8]uril and Blue-Box: High-Energy Water Release Overwhelms Electrostatic Interactions, *J. Am. Chem. Soc.*, 2013, **135**, 14879–14888.

55 J. W. Lee, K. Kim, S. Choi, Y. H. Ko, S. Sakamoto, K. Yamaguchi and K. Kim, Unprecedented host-induced intramolecular charge-transfer complex formation, *Chem. Commun.*, 2002, 2692–2693.

56 A. I. Lazar, F. Biedermann, K. R. Mustafina, K. I. Assaf, A. Hennig and W. M. Nau, Nanomolar Binding of Steroids to Cucurbit[n]urils: Selectivity and Applications, *J. Am. Chem. Soc.*, 2016, **138**, 13022–13029.

57 M. Irie, T. Fukaminato, K. Matsuda and S. Kobatake, Photochromism of Diarylethene Molecules and Crystals: Memories, Switches, and Actuators, *Chem. Rev.*, 2014, **114**, 12174–12277.

58 M. Takeshita, N. Kato, S. Kawauchi, T. Imase, J. Watanabe and M. Irie, Photochromism of Dithienylethenes Included in Cyclodextrins, *J. Org. Chem.*, 1998, **63**, 9306–9313.

59 R. Joseph, A. Nkrumah, R. J. Clark and E. Masson, Stabilization of Cucurbituril/Guest Assemblies via Long-Range Coulombic and CH···O Interactions, *J. Am. Chem. Soc.*, 2014, **136**, 6602–6607.

60 P. Pracht, F. Bohle and S. Grimme, Automated exploration of the low-energy chemical space with fast quantum chemical methods, *Phys. Chem. Chem. Phys.*, 2020, **22**, 7169–7192.

61 C. Lefebvre, H. Khartabil, J.-C. Boisson, J. Contreras-García, J.-P. Piquemal and E. Hénon, The Independent Gradient Model: A New Approach for Probing Strong and Weak Interactions in Molecules from Wave Function Calculations, *ChemPhysChem*, 2018, **19**, 724–735.

62 C. Lefebvre, G. Rubez, H. Khartabil, J.-C. Boisson, J. Contreras-García and E. Hénon, Accurately extracting the signature of intermolecular interactions present in the NCI plot of the reduced density gradient versus electron density, *Phys. Chem. Chem. Phys.*, 2017, **19**, 17928–17936.

63 O. Reany, A. Li, M. Yefet, M. K. Gilson and E. Keinan, Attractive Interactions between Heteroallenes and the Cucurbituril Portal, *J. Am. Chem. Soc.*, 2017, **139**, 8138–8145.

64 S. Moghaddam, C. Yang, M. Rekharsky, Y. H. Ko, K. Kim, Y. Inoue and M. K. Gilson, New Ultrahigh Affinity Host–Guest Complexes of Cucurbit[7]uril with Bicyclo[2.2.2] octane and Adamantane Guests: Thermodynamic Analysis and Evaluation of M2 Affinity Calculations, *J. Am. Chem. Soc.*, 2011, **133**, 3570–3581.

65 C. B. Aakeroy, D. L. Bryce, G. R. Desiraju, A. Frontera, A. C. Legon, F. Nicotra, K. Rissanen, S. Scheiner, G. Terraneo, P. Metrangolo and G. Resnati, Definition of the chalcogen bond (IUPAC Recommendations 2019), *Pure Appl. Chem.*, 2019, **91**, 1889–1892.

66 N. Biot and D. Bonifazi, Chalcogen-bond driven molecular recognition at work, *Coord. Chem. Rev.*, 2020, **413**, 213243.

67 P. Scilabra, G. Terraneo and G. Resnati, The Chalcogen Bond in Crystalline Solids: A World Parallel to Halogen Bond, *Acc. Chem. Res.*, 2019, **52**, 1313–1324.

68 H. S. El-Sheshtawy, B. S. Bassil, K. I. Assaf, U. Kortz and W. M. Nau, Halogen Bonding inside a Molecular Container, *J. Am. Chem. Soc.*, 2012, **134**, 19935–19941.

69 T. Clark, M. Hennemann, J. S. Murray and P. Politzer, Halogen bonding: the σ-hole, *J. Mol. Model.*, 2007, **13**, 291–296.

70 M. Mantina, A. C. Chamberlin, R. Valero, C. J. Cramer and D. G. Truhlar, Consistent van der Waals Radii for the Whole Main Group, *J. Phys. Chem. A*, 2009, **113**, 5806–5812.

71 K. Kříž, J. Fanfrlík and M. Lepšík, Chalcogen Bonding in Protein–Ligand Complexes: PDB Survey and Quantum Mechanical Calculations, *ChemPhysChem*, 2018, **19**, 2540–2548.

72 G. H. Aryal, K. I. Assaf, K. W. Hunter, W. M. Nau and L. Huang, Intracavity folding of a perylene dye affords a high-affinity complex with cucurbit[8]uril, *Chem. Commun.*, 2017, **53**, 9242–9245.

73 F. Biedermann, V. D. Uzunova, O. A. Scherman, W. M. Nau and A. De Simone, Release of high-energy water as an essential driving force for the high-affinity binding of cucurbit[n]urils., *J. Am. Chem. Soc.*, 2012, **134**, 15318–15323.

74 F. Biedermann and H.-J. Schneider, Experimental Binding Energies in Supramolecular Complexes, *Chem. Rev.*, 2016, **116**, 5216–5300.

75 J. E. DeLorbe, J. H. Clements, M. G. Teresk, A. P. Benfield, H. R. Plake, L. E. Millspaugh and S. F. Martin, Thermodynamic and structural effects of conformational constraints in protein-ligand interactions. Entropic paradoxy associated with ligand preorganization, *J. Am. Chem. Soc.*, 2009, **131**, 16758–16770.

76 P. P. N. Syamala and F. Würthner, Modulation of the Self-Assembly of π-Amphiphiles in Water from Enthalpy- to Entropy-Driven by Enwrapping Substituents, *Chem. – Eur. J.*, 2020, **26**, 8426–8434.

77 M. Takeshita, M. Yamada, N. Kato and M. Irie, Photochromism of dithienylethene-bis(trimethylammonium) iodide in cyclodextrin cavities, *J. Chem. Soc., Perkin Trans. 2*, 2000, 619–622.

78 R. N. Dsouza, U. Pischel and W. M. Nau, Fluorescent Dyes and Their Supramolecular Host/Guest Complexes with Macrocycles in Aqueous Solution., *Chem. Rev.*, 2011, **111**, 7941–7980.

79 J. Vázquez, M. A. Romero, R. N. Dsouza and U. Pischel, Phototriggered release of amine from a cucurbituril macrocycle, *Chem. Commun.*, 2016, **52**, 6245–6248.

80 M. A. Romero, P. Mateus, B. Matos, Á. Acuña, L. García-Río, J. F. Arteaga, U. Pischel and N. Basílio, Binding of Flavylium Ions to Sulfonatocalix[4]arene and Implication in the Photorelease of Biologically Relevant Guests in Water, *J. Org. Chem.*, 2019, **84**, 10852–10859.